

The near constant loss dynamic mode in metallic glass

H. Y. Jiang, P. Luo, P. Wen, H. Y. Bai, W. H. Wang, and M. X. Pan

Citation: *Journal of Applied Physics* **120**, 145106 (2016); doi: 10.1063/1.4964809

View online: <http://dx.doi.org/10.1063/1.4964809>

View Table of Contents: <http://scitation.aip.org/content/aip/journal/jap/120/14?ver=pdfcov>

Published by the [AIP Publishing](#)

Articles you may be interested in

[Understanding the changes in ductility and Poisson's ratio of metallic glasses during annealing from microscopic dynamics](#)

J. Appl. Phys. **118**, 034901 (2015); 10.1063/1.4923304

[Effect of physical aging on Johari-Goldstein relaxation in La-based bulk metallic glass](#)

J. Chem. Phys. **141**, 104510 (2014); 10.1063/1.4895396

[The heterogeneous structure of metallic glasses revealed by superconducting transitions](#)

J. Appl. Phys. **114**, 113508 (2013); 10.1063/1.4822018

[Dynamic mechanical analysis in La-based bulk metallic glasses: Secondary \(\$\beta\$ \) and main \(\$\alpha\$ \) relaxations](#)

J. Appl. Phys. **112**, 083528 (2012); 10.1063/1.4759284

[Structural evolution during the sub- \$T_g\$ relaxation of hyperquenched metallic glasses](#)

Appl. Phys. Lett. **96**, 221908 (2010); 10.1063/1.3447373



Pure Metals • Ceramics
Alloys • Polymers
in dozens of forms

Goodfellow

Small quantities *fast* • Expert technical assistance • 5% discount on online orders

The near constant loss dynamic mode in metallic glass

H. Y. Jiang,^{1,2} P. Luo,^{1,2} P. Wen,¹ H. Y. Bai,^{1,2} W. H. Wang,^{1,2,a)} and M. X. Pan^{1,2,a)}

¹*Institute of Physics, Chinese Academy of Sciences, Beijing 100190, China*

²*School of Physical Sciences, University of Chinese Academy of Sciences, Beijing, China*

(Received 20 July 2016; accepted 1 October 2016; published online 13 October 2016)

The near constant loss (NCL) in relaxation spectra is a crucial dynamic phenomenon for glass-forming materials, while its underlying mechanism remains unclear and is hard to study due to the absence of characteristic time scale. We define a characteristic crossover point from both the dynamic mechanical measurements and the quasi-static tension experiments in the metallic glasses (MGs), to study the transition regime, where the NCL dynamics terminates and evolves to the initiation of the β -relaxation. It is found that such transition shows an apparent activation energy well below that of the β -relaxation. Our results also show the concomitant change of the crossover points and the NCL with aging and provide a cursory physical picture on how the NCL occurs, decays and evolves to the β - and α -relaxations in MGs. *Published by AIP Publishing.*

[<http://dx.doi.org/10.1063/1.4964809>]

I. INTRODUCTION

For glassy materials, the relaxation dynamic behavior is usually complex and holds the key to understand their inherent nature of different phenomena and physical and mechanical properties.¹ In comparison to the molecular and polymeric glass-formers, the relaxation spectrum of metallic glasses (MGs) simply made up of atoms^{2,3} is more perspicuous, where there are only two typical kinetic processes: the primary relaxation (α -relaxation) that involves large scale irreversible structural rearrangement and is frozen below the glass transition temperature (T_g) and the secondary relaxation (β -relaxation) in relation to local reversible cooperative motion of atoms of materials that would never vanish with the whole processes.⁴⁻⁷ The researches on MGs have previously found that the β -relaxation,⁸⁻¹³ which is a precursor process of the α -relaxation and correlates with some fundamental issues, such as deformation,¹²⁻¹⁵ aging^{16,17} and diffusions,¹⁸⁻²⁰ generally could be displayed or resolved as a distinct peak in various relaxation spectrums.

Recently, the near constant loss (NCL) rather than a peak shown in relaxation curves at low temperature or high frequency regime has been observed in the glass-forming substances of polyalcohols, polymers, van der Waals molecular glass-formers,²¹⁻²³ ionic conductor materials^{24,25} and metallic glasses²⁶ and even crystalline states,^{27,28} which suggests that the NCL may arise from a fundamental mechanism. For ion conductors, within the framework of the coupling model (CM), the NCL showing weak temperature dependence of the ac conductivity is suggested to originate from the slow decay of cages during a time regime, when there is no mobile ion yet in the glass-formers.^{24,29,30} The mechanism of the NCL for polymers in fast relaxation spectrum is not clear with two possible candidates: the asymmetric double-well potential and the anharmonic models.³¹ Since the NCL process has no characteristic time, it is

difficult to analyze and study its features and properties and figure out its structural origin. Little work has been done on the characteristics and evolution of NCL as well as their relationship with the mechanical and physical properties in MGs. Especially, it is fraught with difficulty to make it clear how the NCL evolves into the β -relaxation, which is of pivotal importance for the in-depth understanding of dynamic behaviors, including the NCL and its correlations with the mechanical and physical properties.

In this paper, we present the investigation on the near constant loss of La₆₀Ni₁₅Al₂₅ metallic glasses using the dynamic mechanical measurements and the quasi-static tension methods. Through defining the crossover points from the NCL contribution to the onset of the β -relaxation as the characteristic temperatures, we show that their apparent activation energy of the NCL can be experimentally determined, which facilitates analyzing the features of the NCL, corroborating the correlation between the NCL and the β -relaxation, and even further triggering a surge of research interest. Our results also show the concomitant change of the crossover points and the NCL with aging durations, which is another perspective for understanding the NCL.

II. EXPERIMENTAL

For the investigation of the rich relaxation dynamics, La₆₀Ni₁₅Al₂₅ MG with excellent glass-forming ability, high thermal stability, and unusual pronounced β -relaxation^{32,33} was utilized. The master alloys were prepared by arc melting of elemental metals with purities above 99.99%, and then MG ribbons were produced by melt spinning. The glassy nature was ascertained by the X-ray diffraction (XRD, a Bruker D8 AA25 diffractometer with the Cu K_α radiation) and a differential scanning calorimeter (DSC, Perkin-Elmer DSC 8000), and the glass transition temperature T_g measured from DSC is 461 K at a heating rate of 20 K/min. The isothermal annealing of samples was conducted at $0.8T_g$ (about 369 K), with samples being sealed in quartz tubes along with high-purity argon gas to avoid oxidation. Both the dynamic

^{a)}Authors to whom correspondence should be addressed. Electronic addresses: whw@iphy.ac.cn and panmx@iphy.ac.cn

mechanical measurements and the quasi-static tensile experiments were performed on a dynamic mechanical analyzer (TA DMA Q800). The dynamic mechanical measurements were conducted in the temperature ramp and frequency sweep mode at a heating rate of 5 K/min, and the quasi-static tensile experiments were used on the specimens at 0.6% tensile strain in the temperature ramp mode at different heating rates. In order to equilibrate samples at the testing temperature, 2 min waiting was applied before the measurements.

III. RESULTS AND DISCUSSION

Figure 1(a) presents the temperature-dependent loss modulus E'' of as-cast $\text{La}_{60}\text{Ni}_{15}\text{Al}_{25}$ MG at a frequency of 8 Hz from a dynamic mechanical measurement. In the temperature range below 300 K, the intensity of loss modulus E'' marked as blue region is kept almost constant, which is called as NCM (near constant modulus).^{21–26} The low and constant intensity of E'' implies that only few defective flow units were activated.¹¹ As temperature advances further, the β -relaxation is gradually triggered and we see a dramatic increase in the loss modulus, which indicates that more flow units with high activation energy are activated. Since NCM has no characteristic time scale, here we define a point of intersection, which is the crossover point of the extended

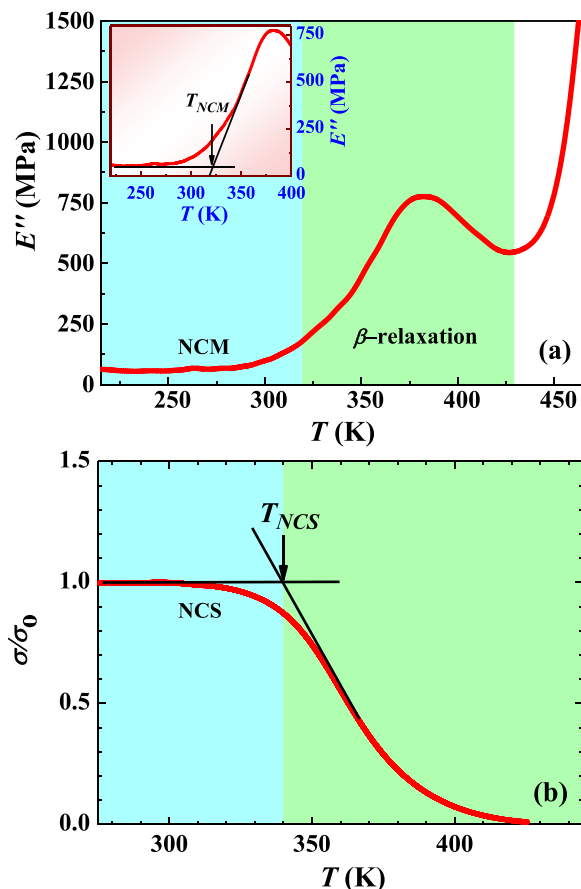


FIG. 1. (a) Temperature dependence of the loss modulus E'' at 8 Hz for as-cast $\text{La}_{60}\text{Ni}_{15}\text{Al}_{25}$ MG. The blue and green regions represent the NCM and the β -relaxation, respectively. (b) The plot of scaled stress against temperature at a heating rate of 1 K/min and constant strain of 0.6%. The blue region represents NCS. T_{NCM} and T_{NCS} are defined as the cross points of the two tangents, as shown in the insets of (a) and (b), respectively.

lines of the NCM and the low temperature side of the β -relaxation peak [see the inset in Fig. 1(a)], as the characteristic temperature T_{NCM} to study its features and correlations with the β -relaxation. A representative experimental curve of the scaled stress against temperature T at a heating rate of 1 K/min and a constant strain of 0.6% for the as-cast sample is shown in Fig. 1(b) from the quasi-static tensile experiment. Unlike the conventional stress relaxation experiments at a constant temperature, the temperature ramp mode stress relaxation utilized here gives more information about the temperature-dependent activation of flow events. Fig. 1(b) shows that the stress is kept almost constant at low temperatures, followed by a dramatic decay as the temperature increases. Being analogous to the loss modulus spectra, we also define the initial stage of the stress relaxation curve as near constant stress (NCS), where the atomic rearrangements are too local to release the stress. A crossover temperature T_{NCS} was specified to characterize the activation of large amounts of flow units [see the inset in Fig. 1(b)]. To express clearly without any confusion, the NCL displayed in the loss modulus spectra and stress relaxation curves are labeled as the two distinct marks, such as NCM and NCS, respectively.

Figure 2(a) shows the temperature-dependent loss modulus E'' spectra of as-cast $\text{La}_{60}\text{Ni}_{15}\text{Al}_{25}$ MG under the discrete testing frequencies, f , ranging from 1 to 16 Hz. The β -relaxation peak shifts to higher temperature for higher frequency, along with a shift of T_{NCM} to higher temperature, as indicated in the inset of Fig. 2(a). Fig. 2(b) plots several representative stress relaxation curves of as-cast samples under different heating rates to investigate the evolution of T_{NCS} with heating rate. The T_{NCS} of different heating rates obtained from the above definition is marked by different color arrows in the plot.

In the glassy materials, an empirical Kissinger equation, $\ln\left(\frac{T_g^2}{\alpha}\right) = \frac{E}{RT} + C$, is usually used to calculate the activation energy E by varying the heating rate α of the measurements. Here, R is the gas constant, T is the characteristic temperature that depends on the heating rate and C is a constant.³⁴ Fig. 3 shows the heating rate dependence of the T_{NCS} plotted in the Kissinger coordinates (the red one). The raw data can be well fitted by the Kissinger relation that gives an apparent activation energy of E_{NCS} around $(13.7 \pm 1.1)RT_g$. The T_{NCM} of dynamic mechanical spectra as a function of frequencies (data obtained from Fig. 2(a)) are also shown in Fig. 3 (data points to the right). Based on the Arrhenius relation, $f = f_\infty \exp(-E/RT)$, where f_∞ is the pre-factor and E is the activation energy,³⁵ the value of E_{NCM} is given to be approximately $(15.5 \pm 1.5)RT_g$, which is close to what obtained from the stress relaxation data. From the similar values of E_{NCS} and E_{NCM} , we infer that the process of the NCM and NCS separately shown in these two different measurements corresponds to identical underlying physical processes, where the initial stage on the stress relaxation curves is related to the NCM on the dynamic spectrum, and the two crossover points reveal the termination of NCL and the beginning of the β -relaxation in MGs. It is noted that the apparent activation energy of the crossover points manifested as the decay of the cages or the onset of the β -

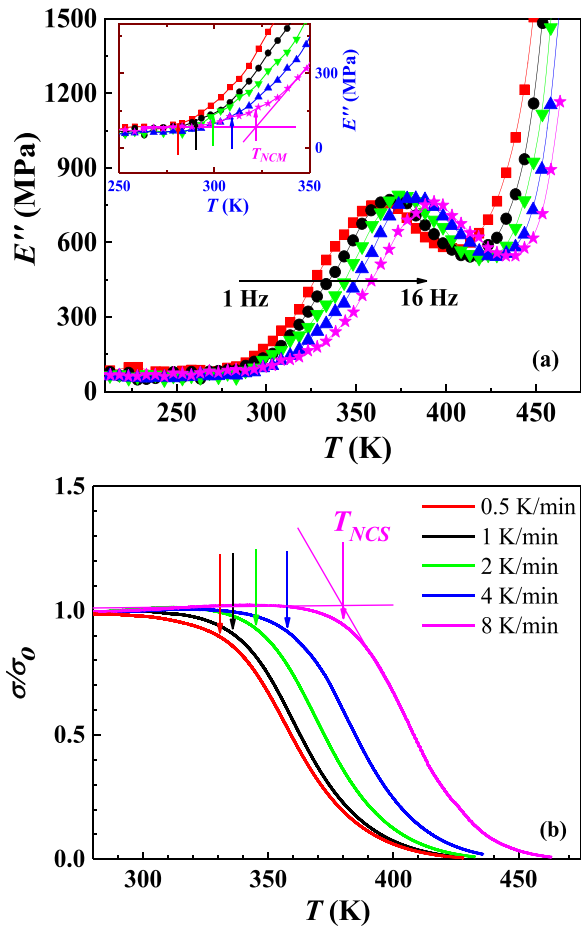


FIG. 2. (a) Temperature dependent loss modulus E'' spectra of as-cast $\text{La}_{60}\text{Ni}_{15}\text{Al}_{25}$ MG with discrete testing frequencies ranging from 1 to 16 Hz. The different T_{NCM} of different frequencies is marked by arrows shown in the inset. (b) The iso-strain stress relaxation curves under different linear heating rates from left to right: 0.5, 1, 2, 4, and 8 K/min. The arrow of corresponding color indicates the T_{NCS} of different heating rates.

relaxation is nearly equivalent to half of that of the β -relaxation E_β ($\sim 26RT_g$), as found in diverse amorphous substances including MGs,^{13,36,37} suggesting the intrinsic correlation between the NCL and the β -relaxation, and its small value with respect to the β -relaxation indicates that the NCL is

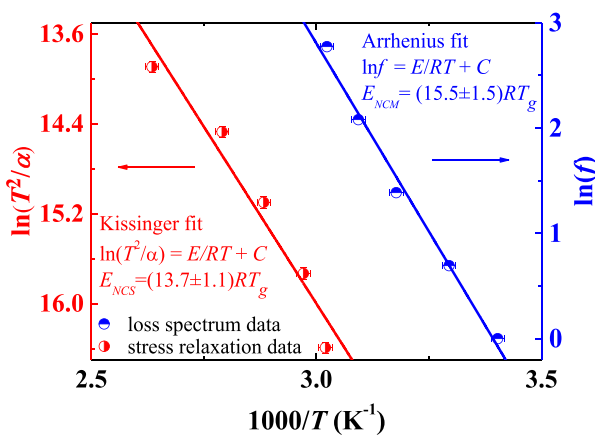


FIG. 3. The blue line is the Arrhenius plot of effective frequencies and the T_{NCM} obtained from Fig. 2(a). Heating rate dependence of the T_{NCS} under different linear heating rates is the red one plotted in the Kissinger coordinates. The value of T_{NCS} can be acquired from Fig. 2(b).

associated with more localized atomic motion than the β -relaxation.^{11,38} This kind of localized atomic motion is even insufficient to release the local stress built by the external applied strain. Interestingly, the activation energy of the fast β -relaxation reported recently is analogous to that of the crossover points signifying the termination of the NCL,³⁹ i.e., both are close to half of E_β , which raises the interest to explore the connection between the NCL and the fast β -relaxation and may

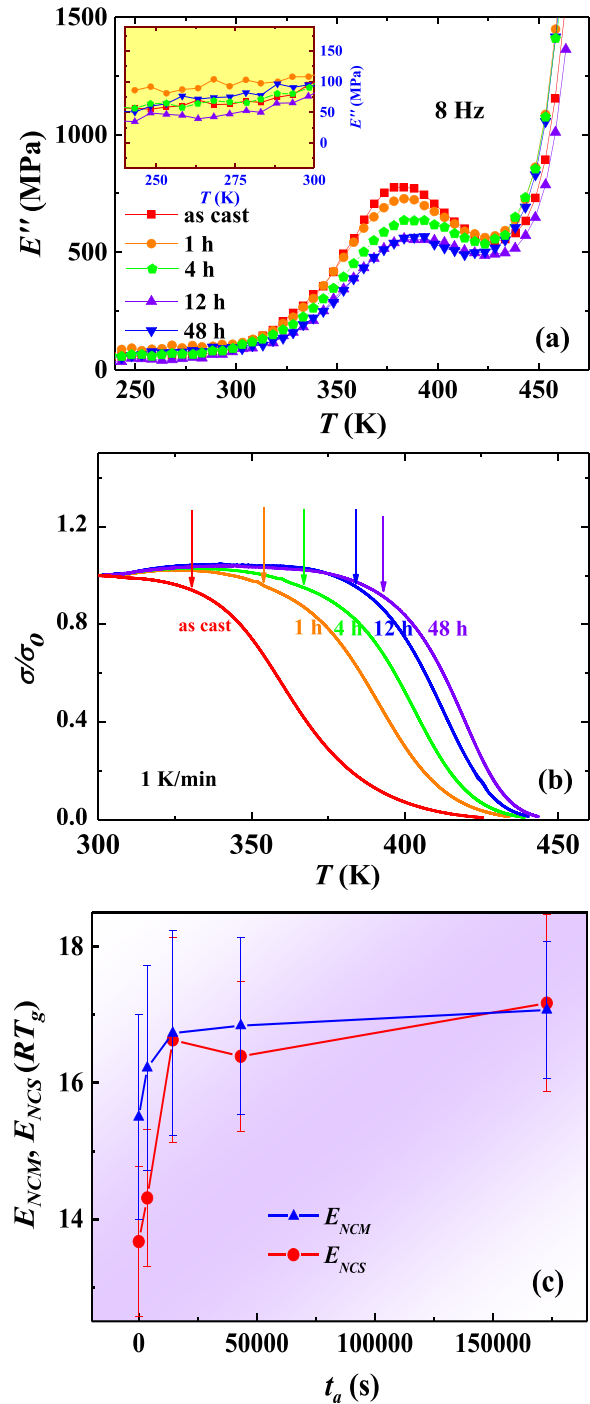


FIG. 4. (a) Loss modulus E'' measured at 8 Hz as a function of temperature T for annealed $\text{La}_{60}\text{Ni}_{15}\text{Al}_{25}$ MG at $0.8T_g$ for 0, 1, 4, 12, and 48 h. The inset shows that the intensity of the NCM almost does not change. (b) The plot of scaled stress against temperature at a heating rate of 1 K/min. (c) The dependence of activation energy measured from two different curves on the annealing time. The calculation methods of the apparent activation energy are illustrated in Figure 3.

facilitate the in-depth understanding of the microscopic mechanism of NCL. The fast β -relaxation is ascribed to the excitation of an individual local event instead of a cascade of local excitations.³⁹ As the NCL and the fast β -relaxation exhibit different behaviors in the relaxation spectra, it is difficult yet to conclude that the NCL and the fast β -relaxation derive from the same microscopic physical origin. More researches are required to distinguish between the rich dynamics of NCL and the fast β -relaxation.

To further investigate the effects of annealing on the crossover points and the NCL, the glass samples were annealed for different times t_a of 1, 4, 12, and 48 h before the measurements at $0.8T_g$, on which temperature the β -relaxation of the specimens is completely activated;³² meanwhile, the crossover points and the NCL show observable changes with aging in the acceptable experimental time window. Figs. 4(a) and 4(b) show the pre-annealing time dependence of the dynamic mechanical spectra at 8 Hz and the stress relaxation curves at a heating rate of 1 K/min, respectively. It can be found that both characteristic temperatures T_{NCM} and T_{NCS} in the two kinds of plots increase with the pre-annealing time. By varying the frequency of dynamic mechanical spectra and the heating rate of stress relaxation measurements, the frequency dependent T_{NCM} and heating rate dependent T_{NCS} for samples with different pre-annealing time can be derived. The characteristic temperatures T_{NCM} under different testing frequencies and T_{NCS} under various heating rates for as-cast and different pre-annealing time samples that are available for fitting the lines analogous to that in Fig. 3 have been listed in Table I. Then, the pre-annealing time dependence of E_{NCS} and E_{NCM} can be obtained, as shown in Fig. 4(c). Both E_{NCS} and E_{NCM} increase with pre-annealing time and are almost equivalent, further confirming that NCL phenomenon was explored from both the dynamical and quasi-static approaches. However, we note that the crossover temperatures, T_{NCS} and T_{NCM} , are somewhat different from each other. This may come from two aspects: on the one hand, the dynamical and quasi-static approaches are more or less different in the way of triggering and responding to flow events; on the other hand, the time scales determined by the applied frequency and heating rate are quite different, thus triggering different flow events

corresponding to different temperatures.⁴⁰ In general, with the increase in the annealing durations, the crossover temperatures of both the types of curves and their corresponding activation energy are growing. It is worth noting that the β -relaxation is a thermal activation process evolving with temperature or time, which means that first the β -relaxation is activated only in the small region with lower activation energy and then its peak in the DMA curves signifies the largest activated area with higher activation energy in the samples. The apparent activation energy of the crossover between the two processes, the NCL and the β -relaxation, implying the termination of the caged atoms dynamics or the onset of the thermally activated β -relaxation, therefore, might be reasonably equivalent to the potential energy barrier that originally confined atoms must overcome to break away from the cages to start cooperatively motion. Based on the findings, we suggest that the NCL stems from highly localized atomic motions existed within individual liquid-like regions of flow units at low temperature.^{11,38} The effects of annealing the MGs could feasibly decrease the fraction of flow units persisted in the entire sample and then reduce the probability of the stochastically activated flow units in low temperature regime. Hence, the apparent activation energy of the crossover points is increased with the augment of annealing time. Moreover, the intensity of the NCM is kept almost unchanged within the experimental sensitivity [see the inset of Fig. 4(a)], which is consistent with the original definition of the near constant loss. Conversely, the intensity of the β -relaxation shows regular decrease with pre-annealing time. The sharp contrast between these behaviors of the NCM and the β -relaxation favors to some extent the previous assumption that the NCM is linked to very extremely local events that are not likely to be affected by the free volume reduction during annealing,⁴¹ whereas the β -relaxation is associated with larger scale atomic motion of flow units that is very sensitive to annealing.⁴²

Based on the above analysis, it is reasonable to suggest that the NCL, as the precursor of the β -relaxation, involves in highly localized atomic motions existed in isolated, stochastic and reversible flow units persisted in the whole metallic glass. The NCL is the caged dynamics decaying with time, and the flow units corresponds to the primitive

TABLE I. Summary of the data of the activation energy E_{NCM} and E_{NCS} , as well as the characteristic temperatures T_{NCM} and T_{NCS} under different testing frequencies (under various heating rates) for as-cast and different pre-annealing time samples.

Annealing time (h)			0	1	4	12	48
Frequency f (Hz)	1	T_{NCM} (K)	294 ± 3	298 ± 3	299 ± 3	299 ± 3	305 ± 3
			303 ± 3	305 ± 3	306 ± 3	307 ± 3	313 ± 3
			315 ± 3	319 ± 3	319 ± 3	320 ± 3	325 ± 3
			323 ± 3	325 ± 3	325 ± 3	326 ± 3	333 ± 3
			331 ± 3	333 ± 3	333 ± 3	334 ± 3	339 ± 3
			331 ± 3	333 ± 3	333 ± 3	334 ± 3	339 ± 3
E_{NCM} (RT_g)			15.5 ± 0.8	16.2 ± 1.0	16.7 ± 1.2	16.8 ± 1.3	17.1 ± 1.0
Heating rate α (K/min)	0.5	T_{NCS} (K)	331 ± 3	350 ± 3	365 ± 3	379 ± 3	383 ± 3
			336 ± 3	362 ± 3	373 ± 3	389 ± 3	390 ± 3
			346 ± 3	365 ± 3	379 ± 3	397 ± 3	400 ± 3
			358 ± 3	378 ± 3	392 ± 3	411 ± 3	413 ± 3
			379 ± 3	404 ± 3	414 ± 3	433 ± 3	435 ± 3
			379 ± 3	404 ± 3	414 ± 3	433 ± 3	435 ± 3
E_{NCS} (RT_g)			13.7 ± 1.1	14.3 ± 1.0	16.6 ± 1.5	16.4 ± 1.1	17.2 ± 1.3

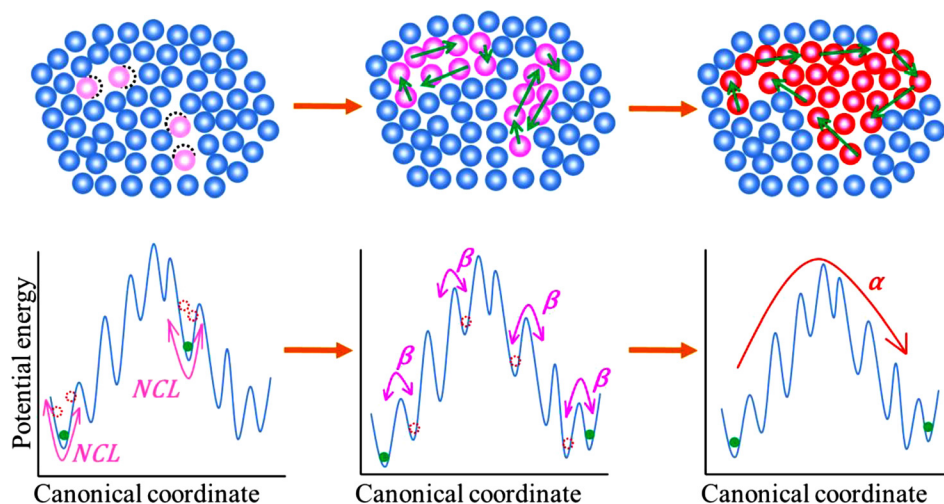


FIG. 5. Two-dimensional schematic of atomic motion of the NCL, β -relaxation and α -relaxation, as well as their relationship (top panel), and the schematic of their corresponding potential energy landscapes (bottom panel). In top panel, the blue and red balls represent elastic matrix and high mobility atoms, respectively. The black dotted line circles and green solid arrows indicate the possible movements of atoms. In bottom panel, the all types of circles represent the possible energy state of MG.

relaxation or Johari-Goldstein β -relaxation, which is the terminator of caged dynamics and the precursor of α -relaxation.^{26,43} The explanation facilitates picturing the evolution of dynamics with temperature changing from the NCL to the β -relaxation and the α -relaxation (see top panel of Fig. 5). After the NCL ended, the next is the onset of the β -relaxation when the more fractions of atoms in the sample can be activated and have a significant potential to leave the cages, with the increase of temperature, and the reversible β -relaxation in which the atoms in flow units has escaped from their own cages and start to cooperate with each other appears and then the flow units are fully activated near T_g , showing the irreversible large scale α -relaxation. To interpret the evolution of dynamics, the corresponding schematic illustration of a potential energy landscape is also shown in Fig. 5. In the NCL regime, particularly, the acquired energy of the high mobility atoms (red balls) confined in the isolated flow units is too low to get over the energy barrier due to the low temperature. When the temperature continues to rise, the highly localized active atoms caged by their nearest neighbors obtain more energy and can jump out of the basins back and forth, and then the β -relaxation occurs. At higher temperature, the irreversible large scale α -relaxation involving more rearranging units appears following the reversible β -relaxation, since the sample can get rid of the megabasins and achieves another energy level.

IV. CONCLUSION

The activation energy of an event normally provides important insight into the underlying mechanism of a dynamic mode. A characteristic crossover point, from both the dynamic mechanical measurements and the quasi-static tension experiments in metallic glasses (MGs), has been defined to describe the transition regime, where the NCL dynamics terminates and evolves to the initiation of the β -relaxation. It is found that such transition shows an apparent activation energy well below that of the β -relaxation. The apparent activation energy of the crossover between the two processes, the NCL and the β -relaxation, implying the termination of the caged atoms dynamics or the onset of

the thermally activated β -relaxation might be reasonably equivalent to the potential energy barrier that originally confined atoms must overcome to break away from the cages to start cooperatively motion. Combining the analyses of the effects of annealing, we further infer that the origin of the NCL exhibited in lower temperature region is extremely local atomic motions existed in isolated, stochastic and reversible flow units persisted in the whole metallic glass. Our work might provide a cursory physical picture on how the NCL occurs, decays and evolves to the β -relaxation in MGs.

ACKNOWLEDGMENTS

We thank Z. Lu, Z. Wang, M. Gao, D. W. Ding, and D. Q. Zhao for insightful discussions and experimental assistance. This work was supported by the NSF of China and MOST 973 Program (No. 2015CB856800).

- ¹J. Y. Cavaille, J. Perez, and G. P. Johari, *Phys. Rev. B* **39**, 2411 (1989).
- ²J. D. Bernal, *Nature* **185**, 68 (1960).
- ³D. B. Miracle, *Nat. Mater.* **3**, 697 (2004).
- ⁴C. A. Angell, K. L. Ngai, G. B. McKenna, P. F. McMillan, and S. W. Martin, *J. Appl. Phys.* **88**, 3113 (2000).
- ⁵P. G. Debenedetti and F. H. Stillinger, *Nature* **410**, 259 (2001).
- ⁶G. P. Johari and M. Goldstein, *J. Chem. Phys.* **53**, 2372 (1970).
- ⁷K. L. Ngai and M. Paluch, *J. Chem. Phys.* **120**, 857 (2004).
- ⁸P. Luo, Z. Lu, Z. G. Zhu, Y. Z. Li, H. Y. Bai, and W. H. Wang, *Appl. Phys. Lett.* **106**, 031907 (2015).
- ⁹J. M. Pelletier, B. Van de Moortèle, and I. R. Lu, *Mater. Sci. Eng., A* **336**, 190 (2002).
- ¹⁰P. Wen, D. Q. Zhao, M. X. Pan, and W. H. Wang, *Appl. Phys. Lett.* **84**, 2790 (2004).
- ¹¹Z. Wang, P. Wen, L. S. Huo, H. Y. Bai, and W. H. Wang, *Appl. Phys. Lett.* **101**, 121906 (2012).
- ¹²H. B. Yu, X. Shen, Z. Wang, L. Gu, W. H. Wang, and H. Y. Bai, *Phys. Rev. Lett.* **108**, 015504 (2012).
- ¹³H. B. Yu, W. H. Wang, H. Y. Bai, Y. Wu, and M. W. Chen, *Phys. Rev. B* **81**, 220201 (2010).
- ¹⁴C. Xiao, J. Y. Jho, and A. F. Yee, *Macromolecules* **27**, 2761 (1994).
- ¹⁵J. S. Harmon, M. D. Demetriou, W. L. Johnson, and K. Samwer, *Phys. Rev. Lett.* **99**, 135502 (2007).
- ¹⁶J. Hachenberg, D. Bedorf, K. Samwer, R. Richert, A. Kahl, M. D. Demetriou, and W. L. Johnson, *Appl. Phys. Lett.* **92**, 131911 (2008).
- ¹⁷R. D. Priestley, C. J. Ellison, L. J. Broadbelt, and J. M. Torkelson, *Science* **309**, 456 (2005).
- ¹⁸K. L. Ngai and S. Capaccioli, *J. Chem. Phys.* **138**, 094504 (2013).
- ¹⁹R. Richert and K. Samwer, *New J. Phys.* **9**, 36 (2007).

- ²⁰H. B. Yu, K. Samwer, Y. Wu, and W. H. Wang, *Phys. Rev. Lett.* **109**, 095508 (2012).
- ²¹S. Capaccioli, K. L. Ngai, M. S. Thayyil, and D. Prevosto, *J. Phys. Chem. B* **119**, 8800 (2015).
- ²²K. L. Ngai, S. Capaccioli, D. Prevosto, and L. M. Wang, *J. Phys. Chem. B* **119**, 12502 (2015).
- ²³K. L. Ngai, S. Capaccioli, D. Prevosto, and L. M. Wang, *J. Phys. Chem. B* **119**, 12519 (2015).
- ²⁴C. Leon, A. Rivera, A. Varez, J. Sanz, J. Santamaria, and K. L. Ngai, *Phys. Rev. Lett.* **86**, 1279 (2001).
- ²⁵W. Bucheli, K. Arbi, J. Sanz, D. Nuzhnyy, S. Kamba, A. Varez, and R. Jimenez, *Phys. Chem. Chem. Phys.* **16**, 15346 (2014).
- ²⁶Z. Wang, K. L. Ngai, W. H. Wang, and S. Capaccioli, *J. Appl. Phys.* **119**, 024902 (2016).
- ²⁷M. R. Díaz-Guillén, M. A. Frechero, J. A. Díaz-Guillén, A. F. Fuentes, and C. León, *J. Electroceram.* **34**, 15 (2015).
- ²⁸A. K. Rizos, J. Alifragis, K. L. Ngai, and P. Heitjans, *J. Chem. Phys.* **114**, 931 (2001).
- ²⁹K. L. Ngai, *J. Chem. Phys.* **110**, 10576 (1999).
- ³⁰A. Rivera, J. Santamaría, C. León, and K. L. Ngai, *J. Phys.: Condens. Matter* **15**, S1633 (2003).
- ³¹A. P. Sokolov, A. Kisluk, V. N. Novikov, and K. Ngai, *Phys. Rev. B* **63**, 172204 (2001).
- ³²Z. Wang, H. B. Yu, P. Wen, H. Y. Bai, and W. H. Wang, *J. Phys.: Condens. Matter* **23**, 142202 (2011).
- ³³H. B. Yu, K. Samwer, W. H. Wang, and H. Y. Bai, *Nat. Commun.* **4**, 2204 (2013).
- ³⁴V. A. Khonik, K. Kitagawa, and H. Morii, *J. Appl. Phys.* **87**, 8440 (2000).
- ³⁵L. M. Martinez and C. A. Angell, *Nature* **410**, 663 (2001).
- ³⁶L. Hu and Y. Yue, *J. Phys. Chem. C* **113**, 15001 (2009).
- ³⁷K. L. Ngai and S. Capaccioli, *Phys. Rev. E* **69**, 031501 (2004).
- ³⁸S. T. Liu, Z. Wang, H. L. Peng, H. B. Yu, and W. H. Wang, *Scr. Mater.* **67**, 9 (2012).
- ³⁹Q. Wang, S. T. Zhang, Y. Yang, Y. D. Dong, C. T. Liu, and J. Lu, *Nat. Commun.* **6**, 7876 (2015).
- ⁴⁰T. P. Ge, X. Q. Gao, B. Huang, W. H. Wang, and H. Y. Bai, *Intermetallics* **67**, 47 (2015).
- ⁴¹A. Slipenyuk and J. Eckert, *Scr. Mater.* **50**, 39 (2004).
- ⁴²P. Luo, Z. Lu, Y. Z. Li, H. Y. Bai, P. Wen, and W. H. Wang, *Phys. Rev. B* **93**, 104204 (2016).
- ⁴³K. L. Ngai, *AIP Conf. Proc.* **708**, 515 (2004).